Supplementary Figures

Supplementary Figure S1. Differential Buoyant Velocity Centrifugation.

A. Breast cancer cell lines (1.2-1.6X10^9) were maintained in Nunc Cell Factories or 15 cm plates. Complete media was replaced with serum-free media containing defined nutrients only. After 5 days in culture, debris was cleared from vesicles and particles by low-speed centrifugation and filtration, and particles and vesicles were harvested using ultracentrifugation. The resulting P70 was sandwiched between a 2.5 M sucrose cushion and a 0.4-2.0 M linear sucrose gradient, and immediately centrifuged for 0-100+ hours at 100,000g. The observed separation of the major particles investigated is illustrated on the right. **B.** One-ml gradient fractions were assessed for weight. The gray bar signifies the typically expected fractions containing exosomes as defined by equilibrium density. **C.** The sucrose concentration was measured by refractometry at the termination of the experiments. The fractions were then assayed for antigenicity and miRNA content. This approach allows separation of different vesicle populations within heterogeneous microvesicle populations, including vesicles with similar buoyant density, such as exosomes and L-exosomes. This approach supplements current methods (86,87) and provided the ability to associate specific surface antigens and miRNA cargo to different particles and structures found within crude exosome preparations gained by ultracentrifugation.

Supplementary Figure S2. Differential Distribution of Neutrally and Selectively Exported MiRNAs Detected by End-Point PCR.

MiRNAs that are exported proportionately to cellular content are labeled as "neutrally released", miRNA species that are selectively exported from malignant cells are labeled as "selectively released".

Supplementary Figure S3. **MiRNAs are exported in similar particles and vesicles from the breast cancer cell line MCF7.**

A. CD81 profile of 6 hour gradients of MCF7 P70s. **B.** Quantitation of indicated miRNAs in fractions using TaqMan qRT-PCR (All data, N=3 of independent experiments, error bars: standard deviation).

Supplementary Figure S4. Vesicular miRNAs are Protected from Ribonucleases.

A. P70 preparations were subjected to filtration through the indicated size cut-off filters prior to buoyancy gradient centrifugation, and specified proteins and miRNA species were measured by fluorescent quantitation or quantitative RT-PCR respectively. **B.** P70 preparations were subjected to Ribonuclease (P70+RNAseA) or mock treatment (P70), and CD81 abundance measured on gradient fractions. **C.** Loss of indicated miRNAs was quantified after ribonuclease treatment before (as exported) or after (purified RNA) Trizol extraction from particles. N=2. Note that miRNA in P70 remained resistant to RNAse, while

added SYNTH RNA was severely degraded. Upon extraction from P70, all miRNAs were degraded by RNaseA. Therefore, all miRNAs that we tested, including nonvesicular miR-1246, are in a form that is protected from RNaseA degradation, confirming that these miRNAs, which we have identified as candidate makers of breast cancer in body fluids (30), are indeed stable miRNA complexes.

Supplementary Figure S5. Ribosomal RNA has a Similar Distribution as miR-1246.

A. MCF7 cells were probed for an rRNA fragment (formerly miR-923, (88), which is also selectively released (30) using miRCURY LNA probes (left panel), and for CD63 using antibodies (right panel); and dyed for DNA. The overlay is shown on in the right panel. Arrows indicate the overlap of the rRNA species with DAPI-negative regions of the nucleus (nucleoli).

Supplementary Figure S6. Blocking Apoptotic Pathways Does not Change Exosome Release.

A. MDA-MB-231 cells were transduced with Bcl-2 and Caspase-9 dominant negative constructs. Three independent stably transduced lines of MDA-MB-231 cells were produced (F, D, A, C, G, B) for the constructs. A vector control expressing GFP was used. The expression of the transgenes was assessed by immunoblotting using anti-FLAG antibody. **B.** The function of the constructs in

these cells to inhibit DNA-damage induced apoptosis was tested by assessing viability upon etoposide treatment. **C.** The profiles of the exosomes released from these cells was quantified by dot-blot analyses using CD81 and normalized to cellular CD81. Each independent cell line was measured twice. **D**. A representative measurement of one of these lines each is shown.

Supplementary References

86. Lasser, C., Eldh, M. and Lotvall, J. (2012) Isolation and Characterization of RNA-Containing Exosomes. Journal of visualized experiments : JoVE.
87. Tauro, B.J., Greening, D.W., Mathias, R.A., Ji, H., Mathivanan, S., Scott, A.M. and Simpson, R.J. (2012) Comparison of ultracentrifugation, density gradient separation, and immunoaffinity capture methods for isolating human colon cancer cell line LIM1863-derived exosomes. Methods.
88. Kozomara, A. and Griffiths-Jones, S. (2011) miRBase: integrating microRNA annotation and deep-sequencing data. Nucleic Acids Res, 39, D152-157.

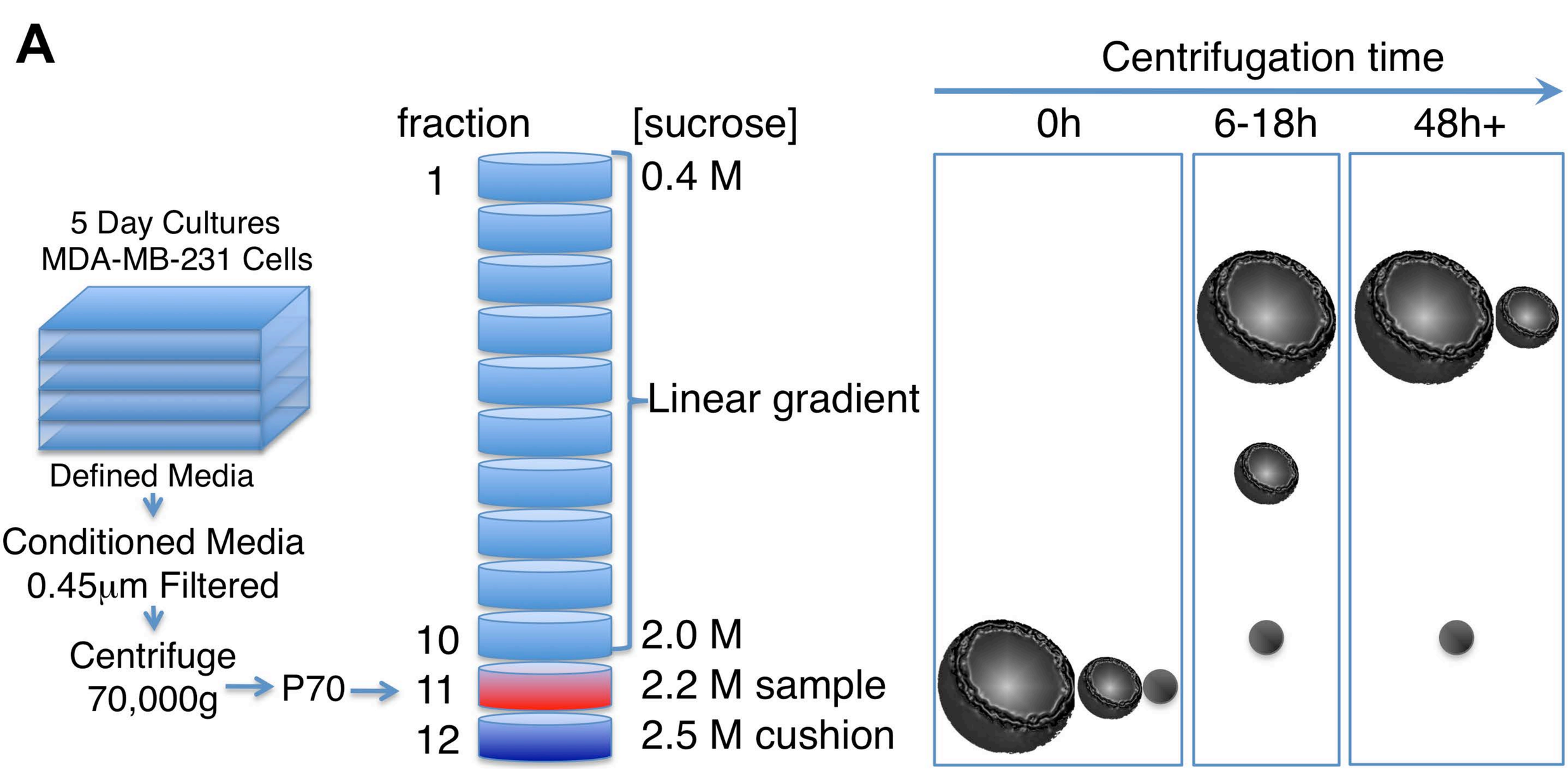

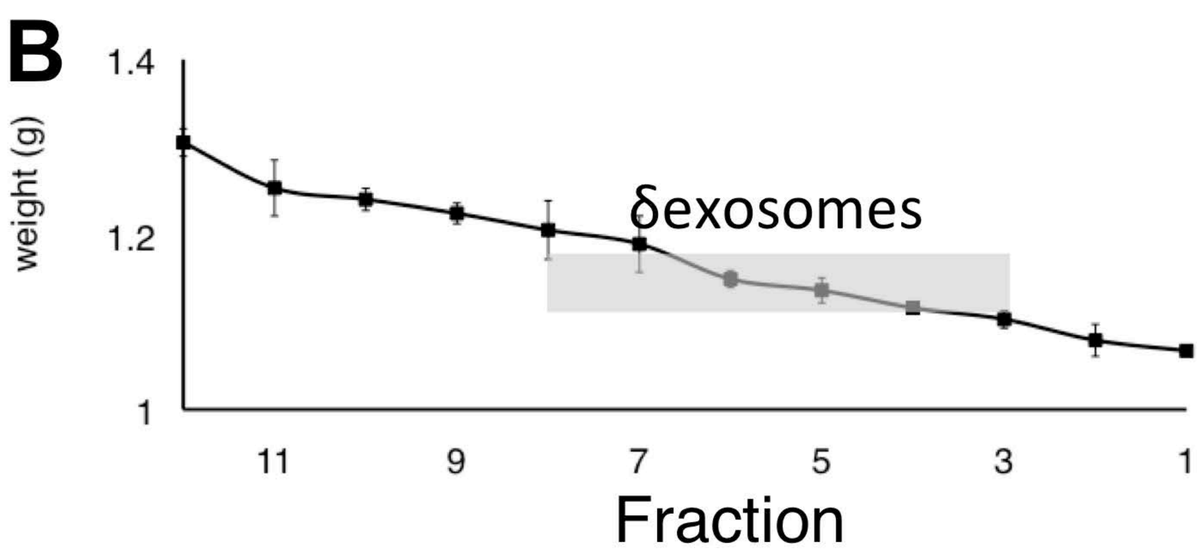

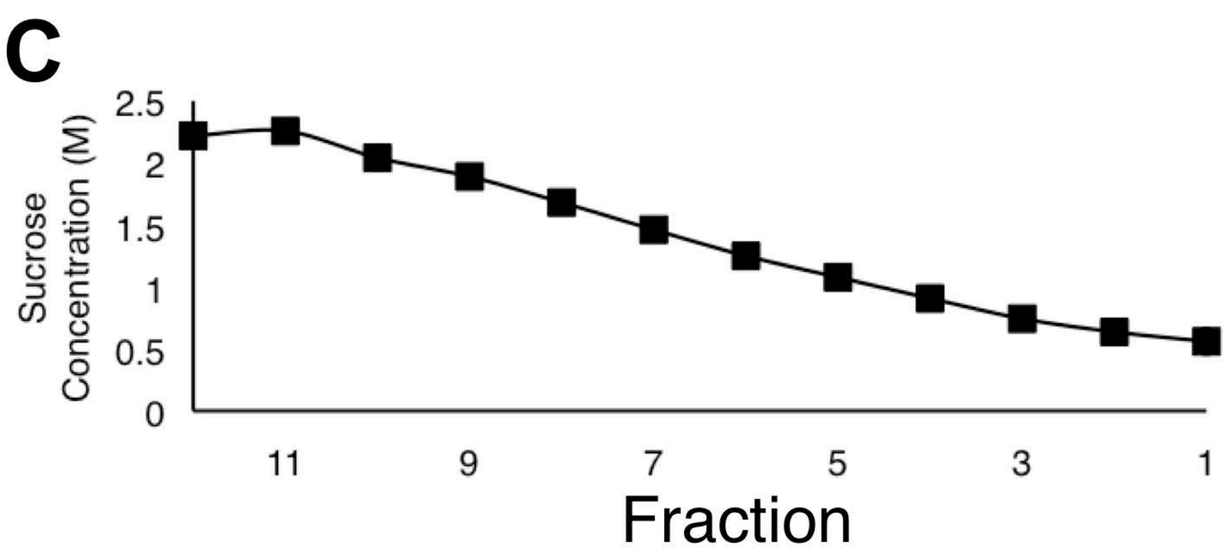

Palma, Yaddanapudi et al. Supplementary Figure S1

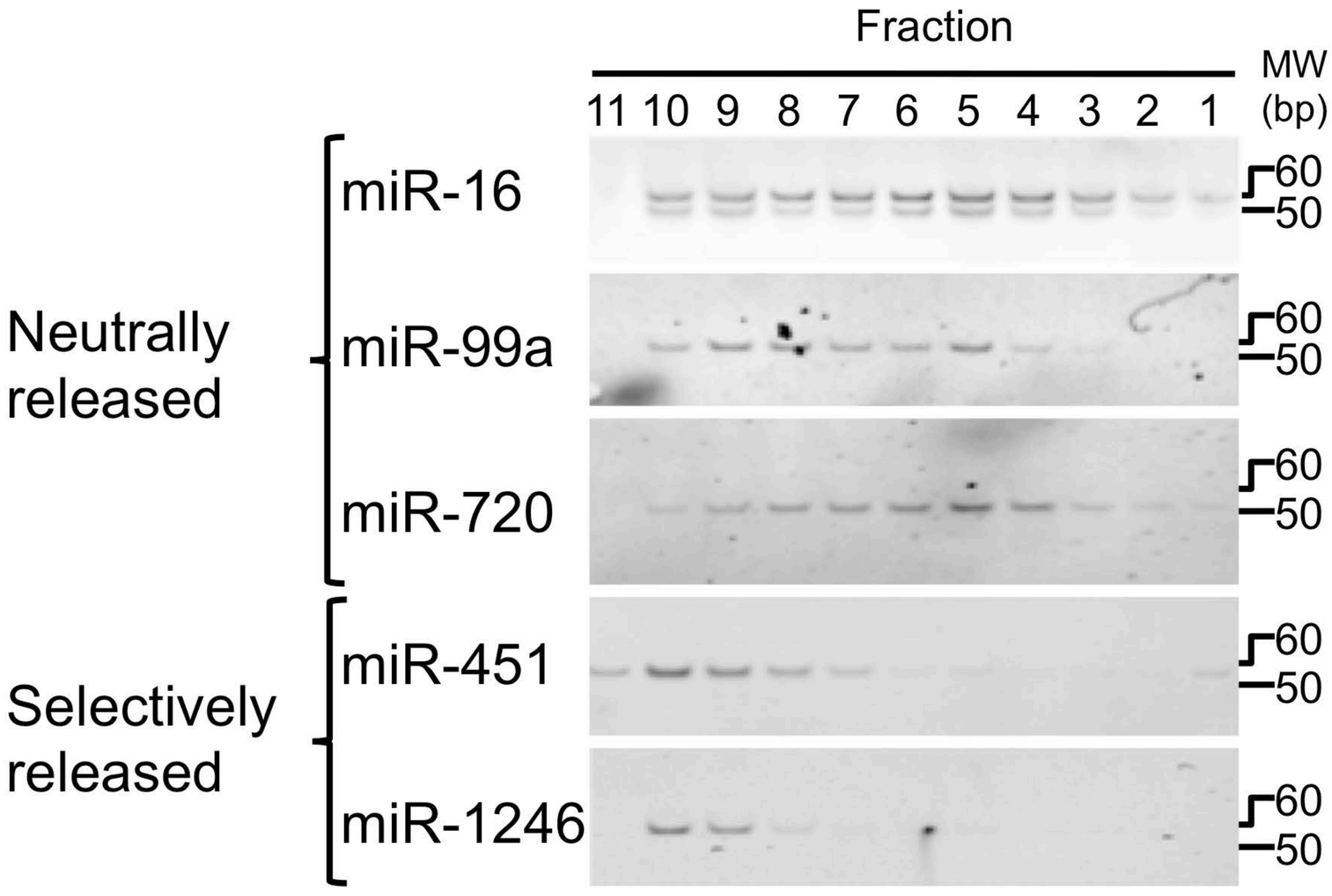

Palma, Yaddanapudi et al. Supplementary Figure S2

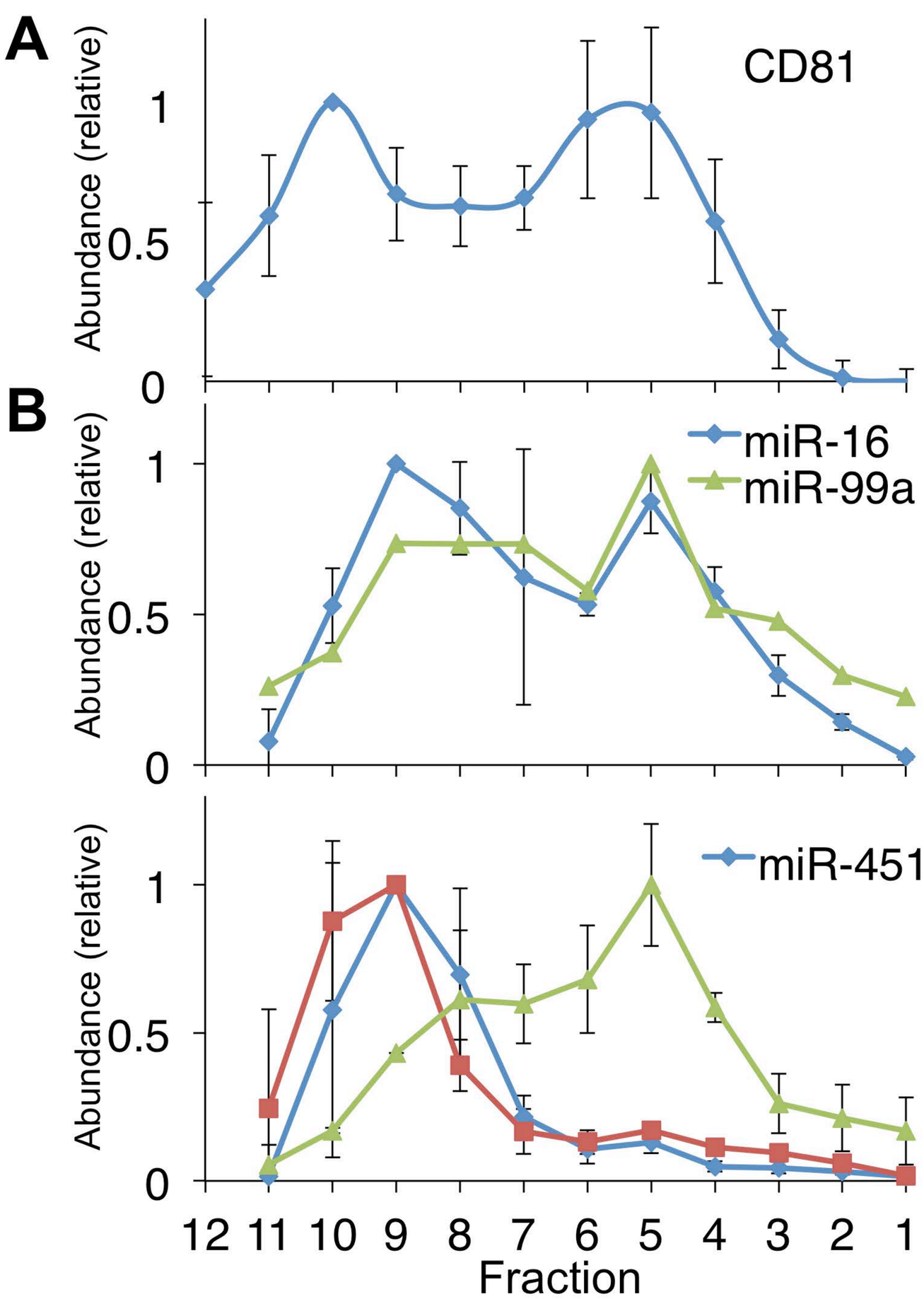

Palma, Yaddanapudi et al. Supplementary Figure S3

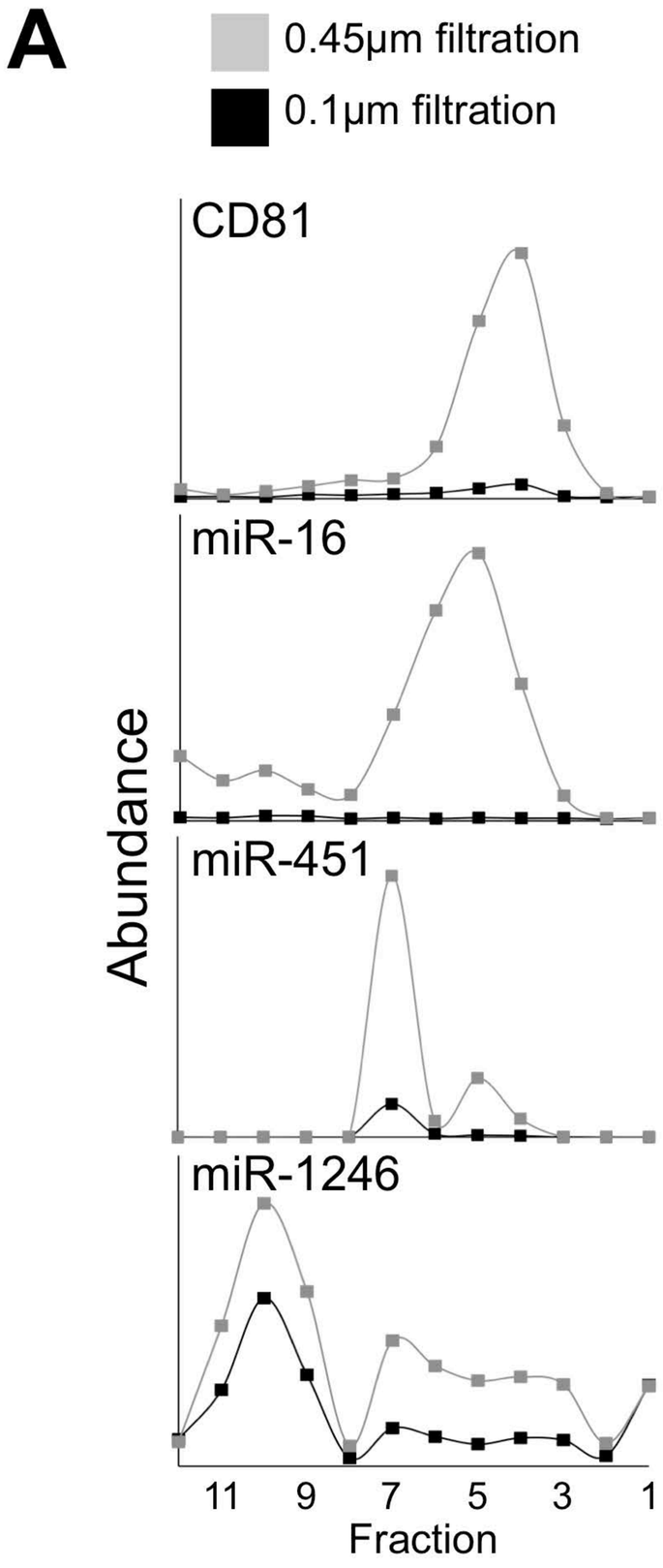

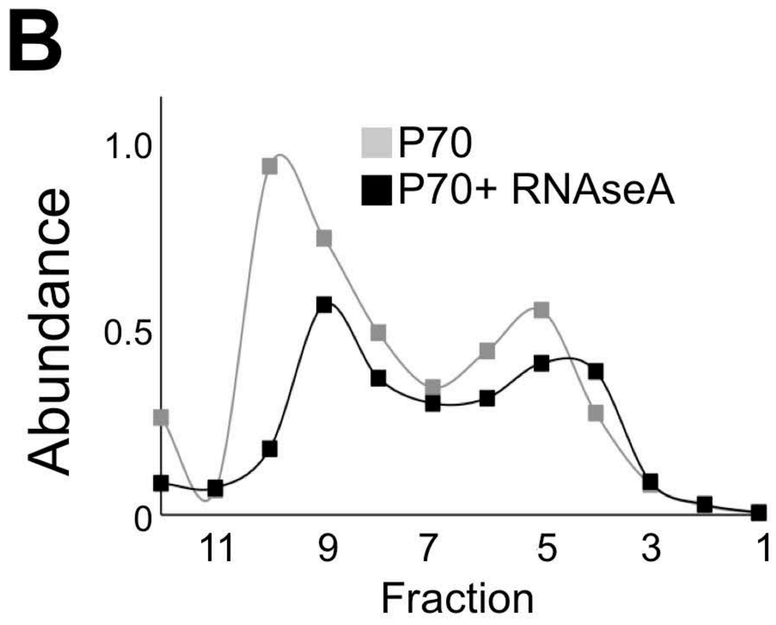

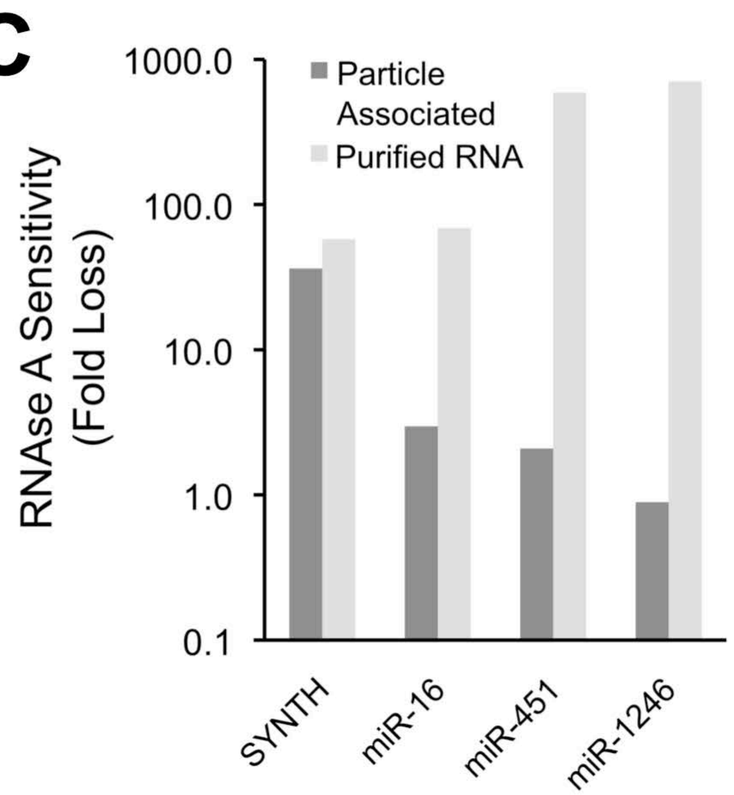

Palma, Yaddanapudi et al. Supplementary Figure S4

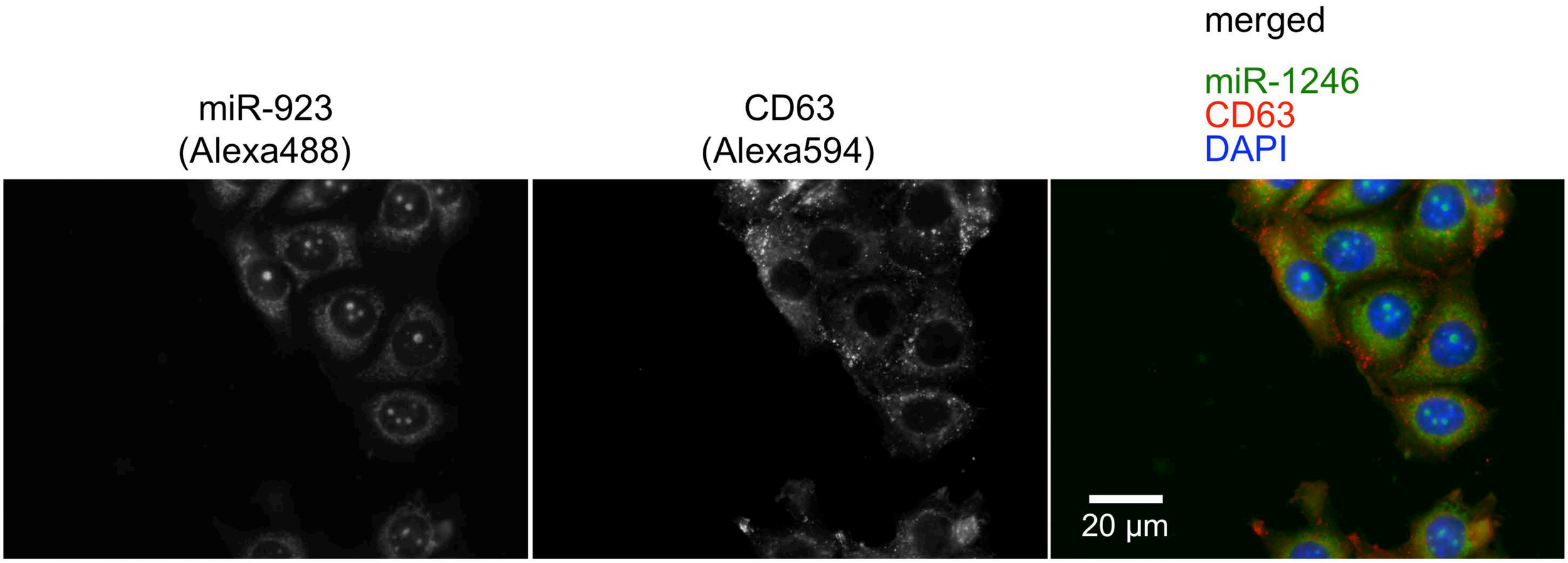

Palma, Yaddanapudi et al. Supplementary Figure S5

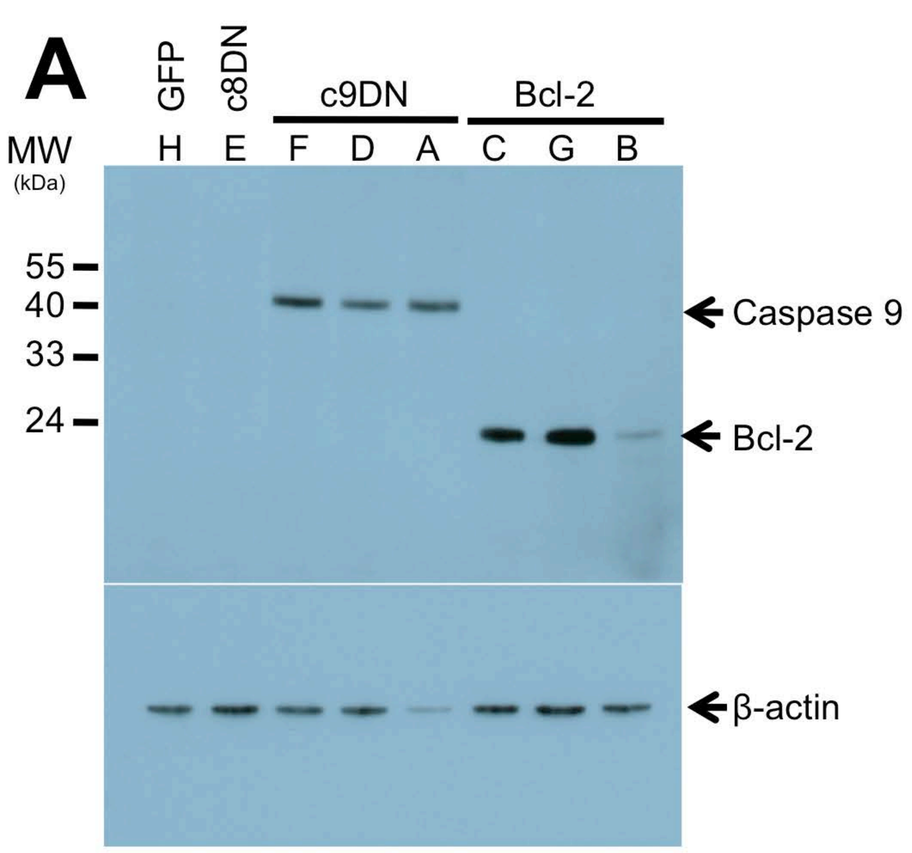

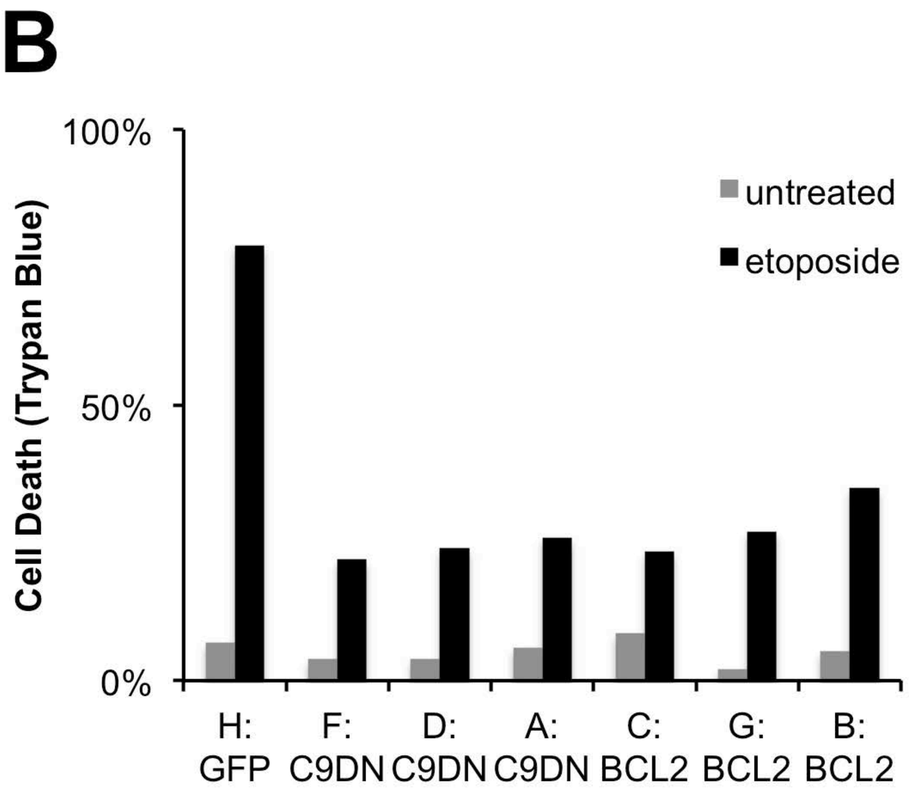

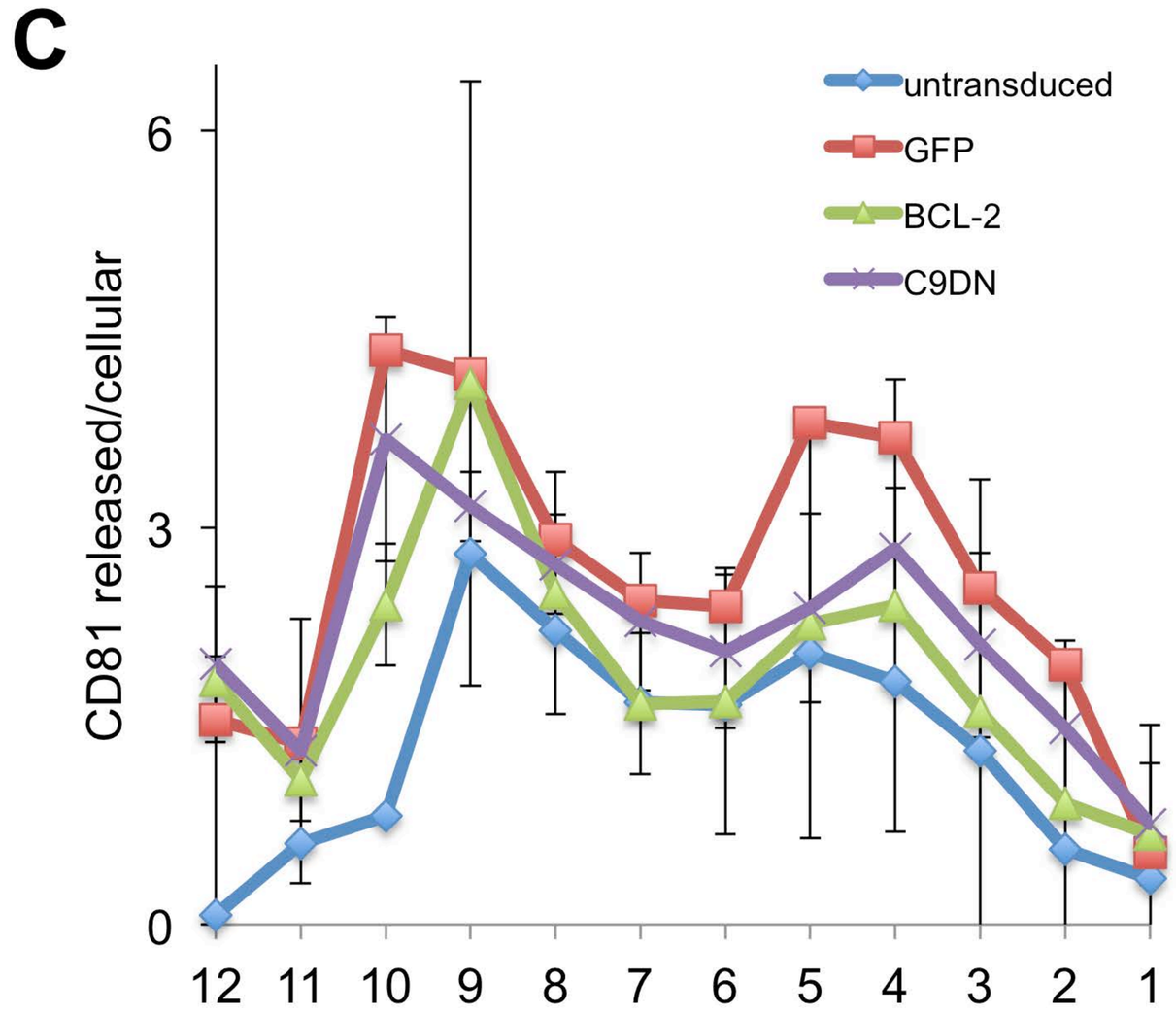

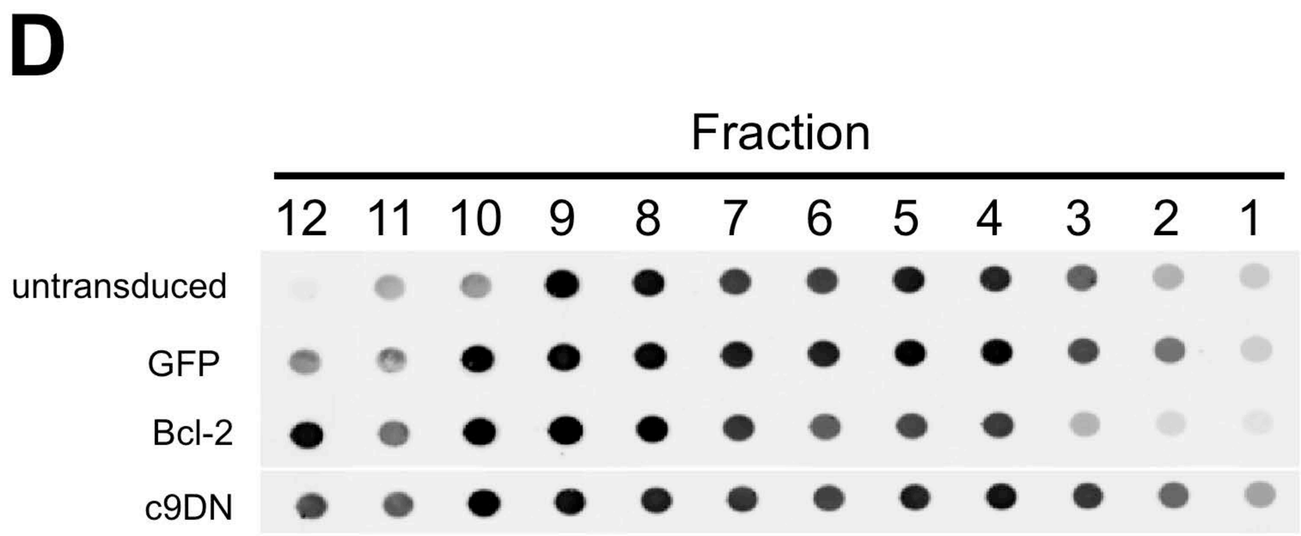

Palma, Yaddanapudi et al. Supplementary Figure S6